Selective field ionization in Li and Rb: Theory and experiment

F. Robicheaux,[1] C. Wesdorp,[2] and L. D. Noordam[2]
[1]*Department of Physics, Auburn University, Auburn, Alabama 36849*
[2]*FOM Institute for Atomic and Molecular Physics, Kruislaan 407, 1098 SJ Amsterdam, The Netherlands*
(Received 7 January 2000; published 13 September 2000)

We present a direct comparison between calculated and measured ionization in Li and Rb when an initially bound Rydberg electron is stripped from the atom by ramping an electric field [0.415 V/(cm ns)]. We describe the method used to calculate the field dependence of the ionization; the method can be used to evolve the population from field strengths where three or more n manifolds cross to the fields where the electron is stripped from the atom. The essential feature of the method is the repeated application of the Landau-Zener approximation for all of the level crossings as the field is ramped. We also give a description of the dynamics of Li and Rb in the ramping field. We observe that the Li selective field ionization is sensitive to the Stark levels within an n manifold, while for Rb only an n dependence is observed.

PACS number(s): 32.60.+i, 32.80.Bx, 31.50.+w

I. INTRODUCTION

Selective field ionization (SFI) has been used as an experimental tool to measure the character and population of highly excited states of atoms and molecules. In SFI, the atom is subjected to an electric field that ramps to higher strengths over times that are very long compared to the classical period of the electron. Eventually the field strength is large enough to rip the electron from the atom. Often the field at which the electron is removed from the atom is when the energy of the state is greater than the classical ionization threshold, in atomic units $E=-2\sqrt{F}$ or equivalently $F=1/16n^4$; in other units, this relationship is often expressed as $E(\mathrm{cm}^{-1})=-6.12\sqrt{F\ (\mathrm{V/cm})}$. We will discuss an interesting violation of this rule below. The signal is the electron current versus field strength (or time); see Refs. [1–8] for early discussions of the process. The technique has been used to characterize the Rydberg population in many different situations: from the collision of slow ions with Rydberg atoms [9] to the zero kinetic energy (ZEKE) [10] states used to measure the rovibrational thresholds of complicated molecules [11]. A feature of this method is that a given initial state will give an electron current with a well-defined distribution in field strength that depends on the ramp rate of the electric field. Because of the long-time scales of the ramp (typically 1 μs) compared to atomic times, no information about relative phases of the excited states is obtained; for example, if the atom is in a wave packet of two states, the SFI signal will be the incoherent sum of the currents from the two states.

This experimental technique is widely used to characterize the population of highly excited states in an atom, but a quantitative, theoretical description of the method does not exist except in the case that after a short ramping period the evolution becomes purely diabatic or adiabatic. In some cases, the lack of a general theory has not impeded the use of SFI, since all aspects could be investigated experimentally or the evolution was nearly diabatic or adiabatic. One obtains the field distributions for specific initial states experimentally by exciting the states with a narrow bandwidth pulsed laser and then ramping the electric field; afterwards, unknown excited-state populations can be charactarized by comparing the resulting field distribution with the previously measured distributions from specific initial states. There are cases where the lack of a theoretical method for calculating an SFI signal has prevented the direct comparison between theory and experiment; often, relevant states cannot be easily excited by a narrow bandwidth pulsed laser.

The purpose of this paper is to present a general method for calculating the SFI signal for a simple atom and to test the method through a quantitative comparison with measured SFI spectra. We are not interested in the field range below the strength needed to mix 3 or more adjacent n manifolds; we consider the evolution in this region to be a solved problem. We are interested in the evolution from the point where several n manifolds are mixed to the point where the electron is stripped from the atom; this problem has been solved only for the extreme cases where the evolution is purely adiabatic or diabatic.

In Fig. 1 we plot the energy levels of $m=0$ levels of Li versus the strength of a static electric field for a simple region near $n=11$ states; m is the eigenvalue of the L_z operator with $\hat{z}$ in the direction of the field. The field strength range is chosen to show how the levels from adjacent n manifolds start to cross as the field strength increases. Suppose that all of the population is in the highest-energy state of the $n=11$ manifold which is marked by an asterisk in Fig. 1. All

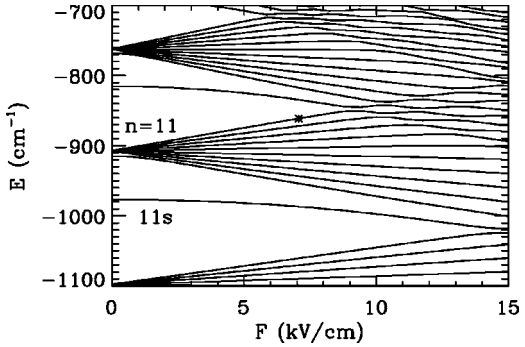

FIG. 1. Energy levels of $m=0$ states of Li as a function of static electric-field strength. These are energies around the $n=11$ manifold.

 ©2000 The American Physical Society

of the population will remain in this state until the field is ramped to ~ 9 kV/cm, where the lowest state from the $n=12$ manifold crosses it. The population can be split among different states at each field strength where levels nearly cross. The amount of population that is on each level can be approximated by a formula from Landau and Zener. For selective field ionization, the population continues through many avoided crossings until reaching a level that is strongly coupled to the continuum, at which point it leaves the atom.

The size of the avoided crossings is crucial for the SFI behavior. The average energy splitting at a crossing is roughly proportional to the sum of the differences of the quantum defects from integers. The Hamiltonian for a hydrogen atom in a static, uniform electric field separates in parabolic coordinates; thus the levels can cross in hydrogen. The levels cannot cross for any other atom due to the deviation from a pure Coulomb potential arising from the core electrons. The deviation from a pure Coulomb potential is reflected in the quantum defects. We have studied two extreme cases in alkali atoms: Li with quantum defects of $\mu_0=0.4$, $\mu_1=0.05$, and $\mu_2=0.002$, and Rb with quantum defects of $\mu_0=3.14$, $\mu_1=2.64$, $\mu_2=1.35$, and $\mu_3=0.02$ (only the non integer parts of the quantum defects are important, giving $\overline{\mu}_0=0.14$, $\overline{\mu}_1=-0.36$, $\overline{\mu}_2=0.35$, and $\overline{\mu}_3=0.02$).

There has been little theoretical work investigating the idea of selective field ionization outside of the extreme cases of purely adiabatic or diabatic evolution when the states from $n+1$ and $n-1$ start to mix. In Refs. [12,13], a model of the crossing of many levels of two adjacent n manifolds was explored; in both papers, all of the crossings were treated within the Landau-Zener approximation, with the difference that the phase accumulation on different paths [14] was neglected in Ref. [12] but incorporated in Ref. [13]. These papers essentially explore the first step of SFI, where the levels of the n manifold start crossing the levels of the $n+1$ manifold.

Simple estimates show why there has been little theoretical work on the general system. If one attempts to perform a brute force numerical integration of Schrödinger's equation, several difficulties soon become apparent. The first is that the electron leaves the atom, so that it is necessary to use a method that will effectively let the electron escape without reflection from unphysical boundaries (either in position space or in basis set space). Once this difficulty is overcome, there is the much more problematic aspect that is related to the relative slowness of the electric-field ramp. For states near $n=50$, the field-free period is roughly 20 ps, which is a factor of 50 000 smaller than the ramping time which is measured in μs. Thus a prohibitively large number of time steps in the numerical integration prevents a direct solution of Schrödinger's equation. Here we have explored an approximation scheme for the calculation of the field distribution of ejected electron current.

The method we have developed was inspired by the treatment in Refs. [12,13], and extends these ideas into a form that can be used to calculate the field distribution. The basic idea is to follow the population through a series of level crossings using the Landau-Zener approximation to obtain the population of each level after a crossing. As in Ref. [12], we ignore the phase accumulation in each path; thus we follow populations instead of amplitudes. This is a very good approximation for SFI once the levels from $n-1$ and $n+1$ start to cross, since there are a very large number of paths that lead to ionization at field F, with nearly randomly varying phases on the different paths; the differing phases essentially guarantee that the interference between different paths will average to zero. In the model of Ref. [13], the phases need to be retained because all of the phase differences were integer multiples of a basic phase difference; this property does not correspond to the actual SFI except in the case where only crossings between n and $n+1$ manifolds are important. Physically our approximation should make sense because the field distribution at which the electron is stripped from the atom is insensitive to the macroscopically small, but on an atomic level huge, variations in ramp rate that are present in every experiment. We have also performed calculations with and without phases, and found negligible differences in the SFI spectrum for the cases we investigated; i.e. the population starts in the region where states from $n-2$ and $n+2$ cross. This paper provides a method for obtaining all the information needed for all Landau-Zener crossings up to the point when the electron leaves the atom.

As a test of the theory, we compared calculated and measured field distributions from states near $n=55$ in Li and Rb; the experiment was constructed so that the initial state was very well characterized. We chose these two atoms to illustrate the different type of SFI spectra that result when the coupling between levels is small (Li) or large (Rb). We excited Li from the $2p_{3/2}$ excited state by a one-photon transition at a specific wavelength with a pulsed, narrow-band dye laser ($\Delta E<0.2$ cm^{-1}). The initial $2p_{3/2}$ was excited by a narrow-band pulsed dye laser ($\Delta E<0.2$ cm^{-1}) laser from the ground state ($2s$), with the polarization perpendicular to the electric field. We varied the wavelength and polarization of the laser that excites the atom from the initial state to the Rydberg states in order to access different Rydberg states. In both experiments, laser power was kept low to avoid an ac Stark shifting of the Rydberg states. The wavelength range was chosen to excite states in zero-field n manifolds from $n=52$ to 55. We also performed SFI measurements and calculations when excitation was performed in a static electric field between 0 and 40 V/cm. Next we performed experiments and calculations in Rb under similar conditions; we excited the Rb atoms from the ground state in a nonresonant two photon process with a narrow-band dye laser $\Delta E<0.2$ cm^{-1}. These variations allowed us to test the theory in many different situations.

II. THEORETICAL METHOD

We first describe the simple theory for SFI when the electron is in a pure Coulomb potential giving a total potential $(-1/r)+Fz$. The Hamiltonian separates in parabolic coordinates ($\xi=r+z$ and $\eta=r-z$) for a static, homogeneous electric field plus Coulomb potential. For the slow ramp rates that are used in SFI, the wave function diabatically evolves so that a state that has n_1 nodes in the up-potential coordinate (ξ) will continue with n_1 nodes. The behavior of the

wave function in the down-potential direction is slightly more complicated. For zero field, the wave function has n_2 nodes in the down-potential coordinate η. Once an electric field is turned on, all states become continuum states, and have an infinite number of nodes in the down-potential direction. This appears to create ambiguities for the definition of the state. However, we can retain conceptual and physical simplicity by noting that the electron starts in the region near the atom and the time to tunnel through the potential barrier is very long on experimental time scales unless the electron has an energy near the top of the barrier. Thus we will define n_2 to be the number of nodes in the down-potential coordinate η in the region between the nucleus and the maximum of the potential. For the slow ramp rates in SFI experiments, n_2 does not change with increasing field. The only parameters that change are the energy and the tunneling rate for a given n_1, n_2. From these ideas, we find that

$$\dot{P}_{n_1 n_2} = -\Gamma_{n_1 n_2}[F(t)] P_{n_1 n_2}, \tag{1}$$

where $P_{n_1 n_2}$ is the population in the n_1, n_2 state, and $\Gamma_{n_1 n_2}[F(t)]$ is the tunneling decay rate which depends on the field strength F at time t. Two general trends to remember: states with $n_1 < n_2$ ($n_1 > n_2$) decrease (increase) in energy with increasing field strength, and states with the same $n_1 + n_2$ decay faster by tunneling as n_2 increases. The tunneling rates are calculated numerically using a WKB approximation [15]; see Refs. [16,17] for discussions of analytic and semiclassical calculations of the tunneling decay.

Our method for calculating the SFI distribution for nonhydrogenic atoms generalizes the simple theory for H in two respects. The first generalization is that the non-Coulombic potential causes couplings between the different n_1, n_2 states; the possibility for population to change quantum numbers when energy levels cross is included through the Landau-Zener approximation. The second generalization is that once the energy of a state is larger than the classical ionization threshold, $-2\sqrt{F}$, it is energetically allowed to escape the atom without tunneling *if* states in closed n_1 channels couple to open channels. This coupling is again mediated through the non-Coulombic potential near the nucleus.

We first describe the generalization due to level crossings. We think of all of the levels as crossing diabatically for the purpose of indexing the states. This is only a bookkeeping device, and does not reflect any choice about the description of the physics. In Fig. 2 we give a schematic drawing of a two-level crossing, and the parameters that characterize the populations before and after the crossing. We define P_1 and P_2 to be populations in states 1 and 2 (respectively) before the crossing, and $\overline{P}_1$ and $\overline{P}_2$ to be the populations after the crossing. We will use A to be the probability that state 1 evolves adiabatically into state 2 after the crossing and D to be the probability that state 1 evolves diabatically into state 1 after the crossing; by symmetry, the probability for 2 to evolve into 1 is A and that for 2 to evolve into 2 is $D = 1 - A$. The conservation of probability demands that $A + D = 1$. Thus after the crossing the populations are

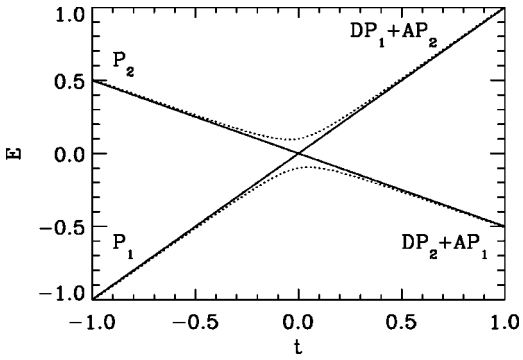

FIG. 2. Schematic drawing of two levels crossing. The solid lines neglect the interaction between the levels, and the dotted lines give the adiabatic energies. Both the time and energy are in arbitrary units. P_1 and P_2 are the original populations. D is the probability to evolve diabatically through the crossing, and $A = 1 - D$ is the probability to evolve adiabatically through the crossing.

$$\overline{P}_1 = DP_1 + AP_2 \quad \text{and} \quad \overline{P}_2 = AP_1 + DP_2. \tag{2}$$

The only difficulty is in calculating A or D and the field dependence of the energies of all the states.

The first step is in obtaining the adiabatic or diabatic transition probabilities in terms of general parameters. Using the Landau-Zener approximation gives the diabatic probability D as

$$D = \exp\left(-2\pi |V_{12}|^2 \Big/ \left| \frac{dE_1}{dt} - \frac{dE_2}{dt} \right| \right), \tag{3}$$

with all parameters evaluated at the crossing; atomic units are used in this equation and throughout the paper unless stated otherwise.

The derivative of the energy with respect to time can be recast as $dE/dt = \dot{F} dE/dF$, where $\dot{F}$ is the ramp rate for the electric field and dE/dF is the derivative of the energy with respect to the field strength. In the calculations, we used the experimental ramp rate of $\dot{F} = 415$ V/(cm μs). The energies are calculated using a WKB approximation [15] by first quantizing the motion in the up-potential coordinate ξ to obtain the separation parameter β_1, and then forcing the phase accumulated between the nucleus and the maximum of the potential to be $(n_2 + 1/2)\pi$ in the down-potential coordinate η. The position of the crossings and dE/dF are obtained numerically from the WKB quantized energy levels. Note that all crossings can be made more diabatic by simply increasing $\dot{F}$, which is an experimentally controllable parameter.

The coupling matrix elements V_{12} can be calculated by using the quantum defects of the zero-field energy levels. First we define a reduced quantum defect $\overline{\mu}_l = \mu_l + j$, where j is an integer such that $-0.5 < \overline{\mu}_l < 0.5$. The effect of the non-Coulombic potential is to shift the energy of the state with energy $-1/2n^2$ by an amount $-\overline{\mu}_l / n^3$; this gives the expectation value of the non-Coulombic potential for energy-normalized Coulomb waves as

$$\int f_l^2(r)V(r)dr = -\overline{\mu_l}. \tag{4}$$

The coupling between energy normalized waves in parabolic coordinates uses the transformation coefficients between the functions in spherical coordinates and parabolic coordinates to give $\overline{V}_{\beta\beta'} = -\Sigma_l U^0_{\beta l} U^0_{\beta' l} \overline{\mu_l}$; U^0 are given by Eqs. (17), (21), and (62) in Ref. [15]. The last remaining task is to convert the functions that are normalized per unit energy to functions that are normalized per unit volume. This is not completely obvious because there are no bound states in the field; as in the definition of the number of nodes in the ξ direction, we only use the part of space from the nucleus to the maximum of the potential in the ξ direction.

With these restrictions, the factor to convert from energy normalization to space normalization is obtained from the energy derivative of the WKB phase between the first two classical turning points in ξ. The conversion factor is $N_\beta^2 = \pi(d\Delta/dE)^{-1}$ given in Eq. (A3) of Ref. [15]; the subscript β indicates the value of the separation constant for the wave function in parabolic coordinates. With these factors, the coupling between two states defined by the separation parameters β and β' is

$$V_{\beta\beta'} = -N_\beta N_{\beta'} \sum_l U^0_{\beta l} U^0_{\beta' l} \overline{\mu_l}. \tag{5}$$

This equation is a generalization of Eq. (4.2) of Ref. [18], which gives the zero field coupling potential between a state from the n manifold and one from the $n+1$ manifold. There is an interesting point of physics that arises from scaling arguments. The rate of change of E depends on the dipole moment, which is proportional to n^2; the coupling matrix element is proportional to $1/n^4$. Thus the evolution of states rapidly becomes diabatic as n increases. This was seen in the experiments of Ref. [4].

The other generalization that needs to be incorporated is the coupling between the ''closed'' channels β_c where the electron needs to tunnel to escape and ''open'' channels β_o where the electron can classically leave the atom. The reason for these two types of channels at the same energy is that the electron can partition its available energy between two different degrees of freedom ξ and η. For $E > -2\sqrt{F}$, the electron can classically leave the atom if the energy is partitioned such that a large enough fraction is in the down-potential η direction. If too much is in the up-potential ξ direction, the electron will have to tunnel to escape. For hydrogen, the energy and motion in the two different directions are uncoupled, and thus the electron *must* tunnel if it is in a closed channel. For all other atoms, the motion in the two different directions are coupled through the non-Coulombic potential from the core electrons, and thus the electron can scatter from a closed channel to an open channel and leave without tunneling.

The possibility of scattering and leaving the atom adds to the decay rate of the state. Using time-dependent perturbation theory, the decay rate to go from a closed channel to an open channel is $\Gamma = 2\pi|V_{oc}|^2$, where the open-channel function is normalized per unit energy and the closed-channel is space normalized. We can use the coupling matrices from above, but now only space normalize the closed function to obtain an additional decay rate

$$\Gamma_c = 2\pi N^2_{\beta_c} \sum_{\beta_o} \left| \sum_l U^0_{\beta_c l} U^0_{\beta_o l} \overline{\mu_l} \right|^2, \tag{6}$$

where the sum over all open channels β_o is necessary to obtain the total decay rate.

These are all of the pieces necessary to calculate when the electron is stripped from the atom. To summarize: (1) At each time step, there is a check to see if two levels cross each other; if there is a crossing the populations are redistributed using the Landau-Zener approximation. (2) A decrease in population can occur by tunneling or by scattering from a closed channel into an open channel; the two decay rates are added incoherently due to the different quantum numbers in the final channels. These steps are repeated until the population on the atom decreases to less than 1% of the original population. The calculations presented in this paper used field steps of 0.2 V/cm; the $m=0$ results for Li were obtained with less than 100 steps for a total of $\sim 2\times 10^4$ crossings, while the $m=2$ results were obtained with roughly 1000 steps for a total of $\sim 5\times 10^4$ crossings. The SFI signal is minus the time derivative of the total population.

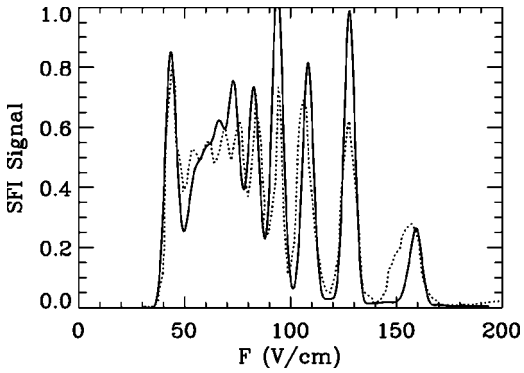

FIG. 3. A comparison between the calculated (solid line) and measured (dotted line) SFI signal for Li excited from the $2p_{3/2}$ state with an energy 39.25 cm^{-1} below the zero field threshold and polarization perpendicular to the electric field. The atom is originally in a static field of 35 V/cm before the field is ramped. The signal is given in arbitrary units.

III. RESULTS

To gauge the effectiveness of this method, we present a comparison between calculated and measured SFI distributions in Li and Rb. In Fig. 3, the measured and calculated SFI spectrum for Li is presented for the case when the second laser excites the atom to an energy of 39.252 cm^{-1} below the zero-field ionization threshold and is polarized perpendicular to the field axis, and the atom is in a 35 V/cm static field at the excitation; this is a typical level of agreement that was achieved between the calculation and experiment. It is clear that all the features are accurately reproduced, and that the approximations work well for this atom.

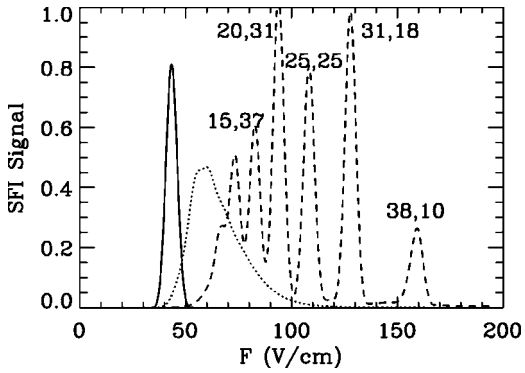

FIG. 4. A separation of the different m components of the calculated SFI signal from Fig. 3: solid line ($m=0$), dotted line ($m=1$), and dashed line ($m=2$). All m components have the same initial central energy and width. Note that the signal for $m=2$ distinguishes the separation of energy between the up- and down-potential directions. The peaks in the $m=2$ spectrum can be classified using the number of nodes, n_1, in the up-potential coordinate and the number of nodes, n_2, in the down potential coordinate with the notation (n_1,n_2,n), where $n=n_1+n_2+|m|+1$; another notation that is sometimes used is the quantum number $k=n_2-n_1$. We have labeled the last five peaks associated with the $m=2$ states using n_1,n_2 notation. Starting from the peak at 160 V/cm to the early peaks at 70 V/cm, the states are (38,10,51), (31,18,52), (25,25,53), (20,31,54), (15,37,55), (11,42,56), and (7,47,57). The last two states are stripped first, and overlap each other near 70 V/cm. At the initial field strength of 35 V/cm, all of these states are within 0.2 cm^{-1} of each other.

The SFI spectrum is a superposition of the spectra from three different final m symmetries: $m=0$, 1, and 2. In Fig. 4, we present the calculated SFI signal from Fig. 3 but separated into m components (the solid line is $m=0$, the dotted line is $m=1$, and the dashed line is $m=2$).

We present a contour plot of the calculated SFI signal versus energy and ramp field for excitation by a photon parallel to the field in Fig. 5 and perpendicular to the field in Fig. 6. In both figures, the excitation was performed in a 35-V/cm static field. These figures show some of the general trends that we observed in the SFI spectra.

There are a number of interesting features of Figs. 3–6 that can be understood at a qualitative level. One important feature is that the excitation laser has a bandwidth of roughly 0.15 cm^{-1}. Thus there are roughly 5–10 Stark states of each

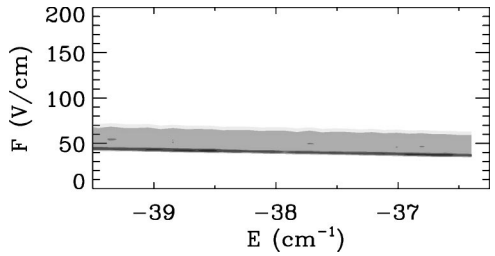

FIG. 5. Contour plot of the calculated SFI signal for Li excited from the $2p_{3/2}$ state with a polarization parallel to the electric field. The atom is originally in a static field of 35 V/cm before the field is ramped.

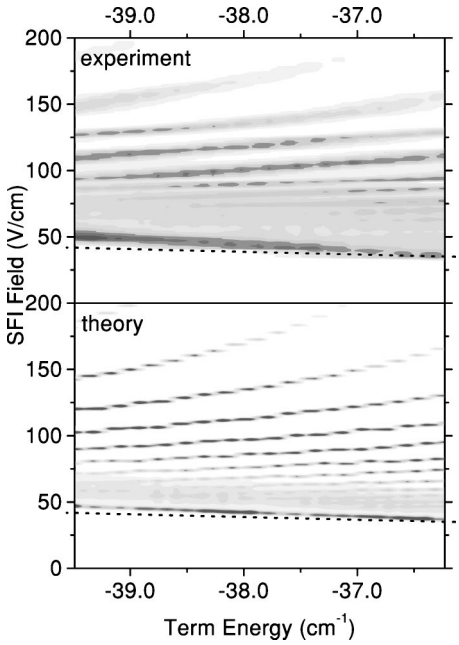

FIG. 6. Experimental and theoretical contour plot of the calculated SFI signal for Li. Same parameters as in Fig. 5, but for perpendicular polarization. The dotted line shows F (V/cm) $=[E\ (cm^{-1})/6.12]^2$.

m component that are initially populated. For fields of $\sim$35 V/cm, the different states that are excited belong to different n manifolds, and have substantially different dipole moments; thus the variation in the division of energy between the two parabolic coordinates is much more substantial than the variation of total energy of the different states.

Another important feature determining the Li SFI spectra is the large difference in quantum defects for the low-l partial waves. The quantum defects are $\mu_0=0.4$, $\mu_1=0.05$, and $\mu_2=0.002$. The differences in quantum defects give quite different behaviors for the different m states in the SFI experiment. The results for a final polarization parallel to the electric field only give final states of $m=0$ and 1 characters for the spatial part of the wave function, since the initial state has $m=0$ and 1 spatial components. We observed somewhat different SFI spectra when we used the $2p_{1/2}$ excited state as the initial state. This is because the composition of the final m states changes due to the different m components of the orbital angular momentum in the $2p_{1/2}$.

These considerations are very important because the different m states behave quite differently in the SFI ramping. The coupling matrix elements depend only on the quantum defect of states with $l \geqslant m$; thus $m=0$ states can couple through $l=0$, 1, and 2 scattering, but $m=2$ states can only couple through $l=2$ scattering. The $m=0$ states go through almost every crossing adiabatically; the large $l=0$ quantum defect provides strong coupling between the different states, because these are the states that suffer most from core scattering. As a result, the population tends to stay on a few levels that are closely grouped in energy. This means that soon after a state has an energy above the classical ionization threshold, $-2\sqrt{F}$, it will scatter into open channels and decay rapidly. Thus the $m=0$ states are in the SFI signal as a

sharp peak at relatively small F. The $m=1$ states evolve largely diabatically, but with a nonnegligible adiabatic interaction at each crossing. Although the purity of the population through each crossing is roughly the same as for $m=0$, the large variation in dipole moments causes the total energy of each state to become quite different. At each crossing, there is a non-negligible probability to mix with states of differing dipole moments, which prevents the total energy differences between the states from becoming as large as in hydrogen. The $m=2$ states evolve almost completely diabatically, and they do not scatter into open channels once the energy is above $-2\sqrt{F}$. Because of the small quantum defects for $l \geqslant 2$, the states only decay once the energy of the n_1, n_2 level can classically decay at which point the electron leaves very rapidly. This case was previously studied, for example, in Ref. [5]. Thus the $m=2$ states give a series of peaks at very separated field strengths which reflects the original partitioning of energy into the up- and down-potential degrees of freedom, and not the total energy of the state that is excited; this is an interesting feature which has not been observed before, to our knowledge.

There are a couple of features in the contour plots of Figs. 5 and 6 that can be interpreted without recourse to extensive calculations. The first obvious feature is that the peak associated with $m=0$ states emerges at smaller F as the energy increases. This occurs because the n levels increase with increasing energy; the $m=0$ states evolve almost purely adiabatically, and their energy hardly changes during the field ramp. The $m=0$ levels are ionized as soon as the field strength is larger than $\sim 1/16n^4$, and are easier to ionize for larger n. Similar considerations hold for the $m=1$ levels; although individual crossings are mainly diabatic, the sheer number of crossings gives an overall spreading of energy without large energy shifts.

The SFI signal from the $m=2$ states display a quite different feature (see Fig. 6). The $m=2$ SFI consists of sharp horizontal bands that move to larger F as the energy increases. The explanation for this phenomenon is somewhat counter intuitive. One band does not correspond to a single state. This can be seen from the part of the bands above 150 V/cm; there it is clear that each band actually consists of short horizontal bands that step up to higher F as the energy increases. The explanation is that each band corresponds to an n manifold. As the energy is increased, the state that is excited in each manifold is at higher energy (see Fig. 1), and thus has a dipole more strongly oriented to the up-potential side of the atom; in other words, states with more nodes in the up-potential coordinate ξ are being excited as the energy increases. These states evolve diabatically for $m=2$, and thus are not stripped until very high field, since the stripping field must increase when more energy is in the up-potential coordinate. The horizontal width of the minibands for $F > 150$ V/cm stems from the laser bandwidth assumed in the calculation.

In Fig. 7, we present a comparison between the experimental and calculated SFI signal for Rb in a 5-V/cm static field to contrast a more standard signal with the Li signal; the ionization yield is peaked near $F=1/16n^4$. The Rb atoms are excited from the ground state using a two-photon, nonresonant transition; the polarization of the laser is perpendicular to the field axis. Both $m=0$ and 2 final states are excited with a ratio of 1:3. For Rb, the quantum defects are large for $l \leqslant 2$, and thus all of the levels cross adiabatically for both $m=0$ and 2; the reduced quantum defects for Rb are $\bar{\mu}_0 = 0.14$, $\bar{\mu}_1 = -0.36$, $\bar{\mu}_2 = 0.35$, and $\bar{\mu}_3 = 0.02$. Thus, for Rb, the SFI signal is not sensitive to which Stark state in the n manifold is excited; the SFI signal is only sensitive to the energy of the state. The Rb SFI can be made to behave more like that for Li by going to higher-n states, ramping the field much faster, or by using an excitation scheme that would access $m=3$ states.

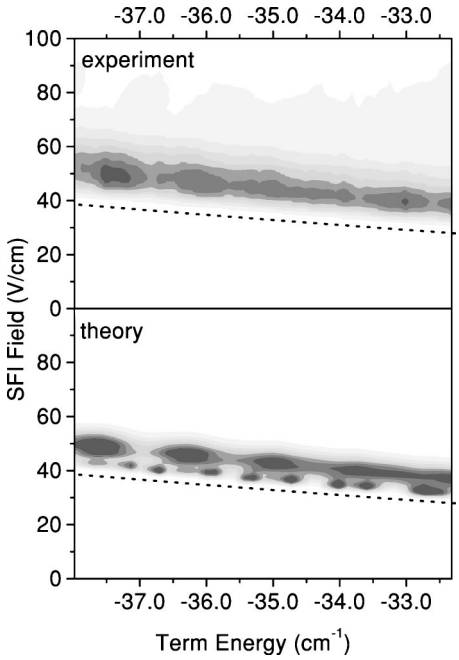

FIG. 7. Experimental and theoretical Rb SFI signal as a function of energy below the zero-field ionization threshold. The Rb is excited in a nonresonant, two-photon transition with the laser polarized perpendicular to the electric field axis. The atom is in a static 5 V/cm field during the excitation. The dotted line shows F (V/cm) $=[E\ (\mathrm{cm}^{-1})/6.12]^2$.

Unlike the Li SFI signal, Rb only shows adiabatic ionization in this energy range and ramp rate. The peak value of F decreases as the energy increases because the electron is easier to remove as its binding energy decreases. Typically, the SFI signal is contained between $(2E/3)^2 > F > (E/2)^2$, when E is measured from the zero-field threshold; as E increases, E^2 and F decrease.

IV. LIMITATIONS OF THE CALCULATION

While our theoretical approach worked well for the cases presented here, there are some easily recognizable situations where the approximations may fail. For example, the approximations may fail if the ramping field does not have a simple form; a ramping field that has an oscillating component could cause trouble by having the phases on different paths become simply related to each other. We stress that we do not propose that the Landau-Zener approximation of this

paper be used when starting from weak fields. The method presented here is meant to evolve the population over a difficult period from when several n manifolds mix to the point where the electron is stripped from the atom. A full SFI theory would use a different technique (perhaps direct propagation of the time-dependent Schrödinger equation) to evolve the system from weak fields to the point where the method in this paper is accurate.

As a contrast, the SFI of ZEKE states should be simply accomplished using the methods described here. The reason for this is that the low-angular-momentum states cannot be strongly populated for the molecule to have long-lived Rydberg states. In typical ZEKE states, this is accomplished by an applied or a stray electric field that mixes the different l states of an n manifold. This is precisely the starting point of these calculations.

The last problem with the proposed method is that it treats every crossing as separate and only involving two levels. There is the possibility for three level crossings once the field becomes larger than $\sim 2/(3n^5)$. Examining the energy map for fields larger than this clearly show many three- and four-crossings that are not *a priori* isolated, although clearly the majority of crossings are isolated two-level crossings. The errors due to treating all crossings as isolated will need to be examined. It is our feeling that multiple crossings play very little role in the SFI signal. The reason for this is that it will take nearly perfect degeneracy between three levels to obtain an effect when the levels evolve mainly diabatically, $D \gg A$; but in this case most of the population will stay in the original state, and thus the errors will be negligible. When the probability for an adiabatic transition A is not small, then the population does not spread far from the adiabatic path; thus most of the population remains within an energy width (determined by the two-level crossings) of the original population and again there will be little error.

V. CONCLUSIONS

In conclusion, we have presented a direct comparison between measured and calculated SFI distributions for Li and Rb. The computational method is an extension of well-known techniques. The main innovation was to use WKB methods to obtain the parameters needed in the evolution of the wave function to the point the electron leaves the atom. We were able to interpret many features of the spectrum. When the atom is excited in a static electric field and the states evolve diabatically, the SFI method is much more sensitive to the division of energy between the two parabolic coordinates than to the total energy of the state. This was the case for Li $m=2$ states presented here; in this situation, the SFI method may be used for a characterization of a state distribution of the Stark levels within an n manifold. This has relevance for ZEKE states. The ZEKE states arise through the mixing of high-l and -m states with the initially excited low-l state; thus the SFI spectrum of ZEKE states should behave most like SFI of hydrogen. Another important finding is that the calculation of SFI distributions for mixed evolution (neither purely diabatic or adiabatic) is not as difficult as had been thought. This technique may be applicable to calculating properties of Rydberg atoms manipulated by other types of time-dependent fields; for example, this method might be useful in calculations of ions scattering from Rydberg atoms.

ACKNOWLEDGMENTS

It is a pleasure to acknowledge discussions with K. B. MacAdam. F.R. was supported by the NSF. Also, this work was part of the research program of the ''Stichting voor Fundamenteel Onderzoek der Materie (FOM),'' which is financially supported by the ''Nederlandse organisatie voor Wetenschappelijke Onderzoek (NWO).''

[1] T.F. Gallagher *et al.*, Phys. Rev. Lett. **37**, 1465 (1976); Phys. Rev. A **16**, 1098 (1977).
[2] J.L. Vialle and H.T. Duong, J. Phys. B **12**, 1407 (1979).
[3] G. Leuchs and H. Walter, Z. Phys. A **293**, 93 (1979).
[4] T.H. Jeys *et al.*, Phys. Rev. Lett. **44**, 390 (1980).
[5] F.G. Kellert *et al.*, Phys. Rev. A **23**, 1127 (1981).
[6] J.H.M. Neijzen and A. Donszelmann, J. Phys. B **15**, L87 (1982).
[7] F.B. Dunning and R.F. Stebbings, *Rydberg States of Atoms and Molecules* (Cambridge University Press, Cambridge, 1983).
[8] K.B. MacAdam, D.B. Smith, and R.G. Rolfes, J. Phys. B **18**, 441 (1985).
[9] L.G. Gray and K.B. MacAdam, J. Phys. B **27**, 3055 (1994).
[10] K. Muller-Dethlefs, M. Sander, and E.W. Schlag, Chem. Phys. Lett. **112**, 291 (1984).
[11] E.W. Schlag, *ZEKE Spectroscopy* (Cambridge University Press, Cambridge, 1998).
[12] D.A. Harmin and P.N. Price, Phys. Rev. A **49**, 1933 (1994).
[13] D.A. Harmin, Phys. Rev. A **56**, 232 (1997).
[14] G.M. Lankhuijzen and L.D. Noordam, Phys. Rev. Lett. **74**, 355 (1995).
[15] D.A. Harmin, Phys. Rev. A **26**, 2656 (1982).
[16] T. Yamabe, A. Tachibana, and H.J. Silverstone, Phys. Rev. A **16**, 877 (1977).
[17] D. Banks and J.G. Leopold, J. Phys. B **11**, L5 (1978).
[18] D.A. Harmin, Phys. Rev. A **30**, 2413 (1984).